Biogeosciences
Discussions

Open Access

EGU

1   # Fate of terrigenous organic matter across the Laptev Sea

2   # from the mouth of the Lena River to the deep sea of the

3   # Arctic interior

4   Lisa Bröder [a,b*], Tommaso Tesi [a,b,c], Joan A. Salvadó [a,b], Igor P. Semiletov [d,e,f], Oleg
5   V. Dudarev [e,f], Örjan Gustafsson [a,b]

6   [a] *Department of Environmental Science and Analytical Chemistry, Stockholm University,*
7   *Stockholm, Sweden*
8   [b] *Bolin Centre for Climate Research, Stockholm University, Stockholm, Sweden*
9   [c] *Institute of Marine Sciences – National Research Council, Bologna, Italy*
10   [d] *International Arctic Research Center, University Alaska Fairbanks, Fairbanks, USA*
11   [e] *Pacific Oceanological Institute, Russian Academy of Sciences, Vladivostok, Russia*
12   [f] *Tomsk National Research Politechnical University, Tomsk, Russia*

13   *corresponding author: lisa.broder@aces.su.se

14 **Abstract**

15 Ongoing global warming in high latitudes may cause an increasing supply of permafrost-

16 derived organic carbon through both river discharge and coastal erosion to the Arctic

17 shelves. Here it can be either buried in sediments, transported to the deep sea or degraded

18 to CO_2 and outgassed, potentially constituting a positive feedback to climate change.

19 This study aims to assess the fate of terrestrial organic carbon (TerrOC) in the Arctic marine

20 environment by exploring how it changes in concentration, composition and degradation

21 status across the wide Laptev Sea shelf. We analyzed a suite of terrestrial biomarkers as

22 well as source-diagnostic bulk carbon isotopes ($\delta^{13}C$, $\Delta^{14}C$) in surface sediments from a

23 Laptev Sea transect spanning more than 800 km from the Lena River mouth (~10 m water

24 depth) across the shelf to the slope and rise (2000-3000 m water depth). These data provide

25 a broad view on different TerrOC pools and their behavior during cross-shelf transport. The

26 concentrations of lignin phenols, cutin acids and high-molecular weight (HMW) wax lipids

27 (tracers of vascular plants) decrease by 89-99 % along the transect. Molecular-based

28 degradation proxies for TerrOC (e.g., the carbon preference index of HMW lipids, the HMW

29 acids/alkanes ratio and the acid/aldehyde ratio of lignin phenols) display a trend to more

30 degraded TerrOC with increasing distance from the coast. We infer that the degree of

31 degradation of permafrost-derived TerrOC is a function of the time spent under oxic

32 conditions during protracted cross-shelf transport. Future work should therefore seek to

33 constrain cross-shelf transport times in order to compute a TerrOC degradation rate and

34 thereby help to quantify potential carbon-climate feedbacks.

Biogeosciences
Discussions
Open Access
EGU

1   Introduction

35

36   Amplified global warming in high latitudes has raised growing concern about potential

37   positive carbon-climate feedbacks. Arctic soils store about half of the global soil organic

38   carbon (Tarnocai et al., 2009), with 60 % of this in perennially frozen grounds (Hugelius et

39   al., 2014). With ongoing climate change these vast carbon reservoirs become increasingly

40   vulnerable. Mobilization and transport of old terrigenous organic carbon (TerrOC) into the

41   Arctic Ocean is expected to intensify (Gustafsson et al., 2011) through enhancing river

42   discharge (McClelland et al., 2008) with augmenting sediment loads (Gordeev, 2006;

43   Syvitski, 2002) and accelerating coastal erosion (Günther et al., 2013). This material can be

44   buried in the sediments of the Arctic shelves, transported across the margin towards deeper

45   basins or degraded and re-introduced into the modern carbon cycle as CO_2, thereby not only

46   providing a potential positive feedback to global warming, but also causing severe ocean

47   acidification (Semiletov et al., 2016). The fate of permafrost-released TerrOC in the marine

48   environment is thus crucial for future climate projections, yet insufficiently understood (Vonk

49   and Gustafsson, 2013).

50   The East Siberian Arctic Shelf (ESAS) is with a width of > 800 km the world's largest

51   continental shelf. It receives TerrOC both from the erosion of the East Siberian shoreline,

52   largely consisting of organic-rich, late-Pleistocene ice-complex deposits (Yedoma), and via

53   the Great Russian Arctic Rivers, which drain extensive areas of continuous and

54   discontinuous permafrost. The Laptev Sea is a representative for the TerrOC dominated

55   Siberian shelf seas, since its main organic carbon input originates from substantial coastal

56   erosion (as observed in the Buor-Khaya Bay, Sánchez-García et al., 2011; Semiletov et al.,

57   2011; Vonk et al., 2012) and the Lena River, the main fluvial sediment source for the entire

58   ESAS (Holmes et al., 2002).

59   Previous studies have focused on near-shore areas and the inner shelf (e.g. Bröder et al.,

60   2016; Charkin et al., 2011; Feng et al., 2015; Karlsson et al., 2011; Salvadó et al., 2015;

61   Sánchez-García et al., 2011; Semiletov et al., 2005, 2012; Tesi et al., 2014; Winterfeld et al.,

62   2015b, 2015a; Vonk et al., 2010, 2012, 2014). They reported large fractions of old TerrOC in

63   particulate organic carbon (POC) and surface sediments close to the coast, using different

64   approaches such as applying carbon-isotope-based source apportionment (e.g. (Gustafsson

65   et al., 2011; Semiletov et al., 2005; Vonk et al., 2010, 2012, 2014) and by analyzing

66   terrigenous biomarkers in both surface sediments (e.g. Feng et al., 2013; Stein and

67   Macdonald, 2004; Tesi et al., 2014, 2016) and POC in the water column (e.g. Charkin et al.,

68   2011; Karlsson et al., 2011; Winterfeld et al., 2015a). This is the first study that encompasses

69   sampling stations along the entire transect from the Lena River mouth, across the wide

70   Laptev Sea shelf, to the continental slope and rise. Our major objective was to gain new

71   insights in the behavior of different TerrOC pools, in particular investigating potential

72   degradation of permafrost-released material along the land-shelf-basin continuum. We have

73   therefore characterized TerrOC in surface sediments along the Laptev Sea transect on both

74   bulk and molecular level, exploiting source-diagnostic bulk carbon isotopes (δ^{13}C, Δ^{14}C) as

75   well as an extensive biomarker suite (lignin phenols and cutin acids obtained by alkaline CuO

76   oxidation and high-molecular-weight solvent-extractable lipids, such as *n*-alkanes and *n*-

77   alkanoic acids).

2 Material and Methods

2.1 Study area

The Laptev Sea is the shallowest of the Arctic shelf seas with an average depth of 48 m

(Jakobsson et al., 2004). It spans over 498,000 km^2 with a volume of 24,000 km^3 and is

located between the Kara Sea and Severnaya Zemlya in the West and the East Siberian Sea

and the New Siberian Islands in the East. The main sources of particulate organic carbon

(POC) for the Laptev Sea are terrigenous, both from coastal erosion and river runoff

(Sánchez-García et al., 2011; Stein and Macdonald, 2004). Marine primary production is

limited to on average two ice-free months per year and therefore generally low. Nutrient-poor

waters on the Siberian shelves resulting from a strong stratification further impede

phytoplankton growth (Sakshaug, 2004).

The destabilization of Pleistocene Ice-Complex Deposits along the coastline is a main

sediment source for the Laptev Sea (Rachold et al., 2000). The total POC input from coastal

erosion to Laptev and East Siberian Sea is estimated to be between 4.0 Tg yr^{-1} (Semiletov,

1999; Stein and Fahl, 2000) and 22 ± 8 Tg yr^{-1} (including net subsea permafrost-carbon

erosion, Vonk et al., 2012).

The Lena River is estimated to provide 20.7 Tg of sediment per year to the Laptev Sea

(Holmes et al., 2002) with an average water discharge of 588 km^3 yr^{-1} (Holmes et al., 2012).

It drains a watershed of ~2.46 x 10^6 km^2 (Holmes et al., 2012), of which 77 % is underlain by

continuous permafrost (Amon et al., 2012). Water discharge peaks in June, during the spring

flood, when about 75 % of total organic carbon is delivered (Rachold et al., 2004). Total POC

discharge by the Lena River can be up to 0.38 Tg yr^{-1} (Semiletov et al., 2011).

Sediment transport pathways are largely influenced by the prevailing atmospheric conditions:

During cyclonic summers (i.e. positive phase of the Arctic Oscillation), northerly winds

predominate, strengthening the Siberian Coastal Current, which transports Lena River water

masses along the coast towards the East Siberian Sea; whereas during anticyclonic

summers (i.e. negative phase of the Arctic Oscillation and mainly southerly winds) the Lena

River plume is exported onto the mid-shelf and towards the deep part of the Arctic Ocean

106   (Charkin et al., 2011; Dmitrenko et al., 2008; Guay et al., 2001; Wegner et al., 2013;

107   Weingartner et al., 1999). Sediment transport in the Laptev Sea is strongly seasonal. The

108   main transport of Lena River water with high concentrations of suspended particulate matter

109   (SPM) towards the mid-shelf takes place shortly after river-ice breakup (Wegner et al., 2005).

110   During the ice-free summer, SPM circulates between inner and mid-shelf with very little

111   material escaping over the shelf break to the deeper parts of the Arctic Ocean. Significant

112   sediment export is suggested to happen during freeze-up through SPM that is incorporated

113   in sea ice and then transported across the continental margin (Dethleff, 2005; Eicken et al.,

114   1997) or through the formation of dense bottom water resulting from brine ejection (Dethleff,

115   2010; Ivanov and Golovin, 2007). Hardly any sediment transport occurs beneath the ice

116   cover.

117   Holocene-scale linear sedimentation rates for the Laptev Sea vary between 0.12 and 0.59

118   mm yr^{-1} according to ^{14}C dating of marine bivalves (Stein and Fahl, 2004, and citations

119   therein), whereas centennial-scale ^{210}Pb-derived rates for the more recent Laptev Sea can

120   be up to 1.3 mm yr^{-1} (Vonk et al., 2012). These rates do not seem to be correlated with water

121   depth on the shelf, but values for the continental slope and rise tend to be on the lower end

122   (0.12-0.38 mm yr^{-1}) (Stein and Fahl, 2004, and citations therein).

123

124   2.2 Sampling

125   Sediment sampling locations span from close to the Lena River mouth and in the Buor-

126   Khaya Bay, across the shelf, to the continental slope and rise, covering a transect of > 800

127   km with water depths increasing by more than two orders of magnitude. Samples SW-1, SW-

128   2, SW-3, SW-4, SW-6, SW-14, SW-23 and SW-24 were collected during the SWERUS-C3

129   expedition on IB *ODEN* during summer 2014 using an Oktopus multicorer (8 Plexiglas tubes,

130   10 cm diameter). All other samples were collected during the International Siberian Shelf

131   Study (ISSS-08) expedition onboard the RV *Yacob Smirnitskyi* during summer 2008. The

132   YS-4, YS-6, YS-13 and YS-14 samples were taken with a GEMAX gravity corer (2 Plexiglas

133   tubes, 9 cm diameter); YS-9 and TB-46 were collected with a Van Veen grab sampler. For

134   the grab samples only surface sediments (uppermost cm) were subsampled and used in this

135   study. Sediment cores were cut into 1 cm slices within 24 hours after sampling. To account

136   for lower sediment accumulation rates on the rise, for SW-1, SW-2, SW-3 and SW-4 a higher

137   resolution of 0.5 cm for the top 10 cm was chosen. The depositional age for all samples is

138   thus between ~8 and ~70 years (depending on which sedimentation rates are employed). All

139   samples were kept frozen throughout the expedition and freeze-dried upon arrival. See

140   Semiletov and Gustafsson (2009) for more information on the ISSS-08 expedition. For exact

141   sampling locations see Table 1.

142

143   2.3 Surface area

144   All surface area analyses have been performed on a micromeritics Gemini VII Surface Area

145   and Porosity analyzer. Freeze-dried subsamples of ~0.7 g were furnaced at 400 °C for 12 h

146   and gently cooled down to room temperature. They were then desalted by repeated mixing

147   with 50 ml of MilliQ water and centrifugation (20 min at 8000 rpm), followed by further freeze-

148   drying. Directly prior to analysis they were degassed in a Micromeritics FlowPrep 060

149   Sample Degas System for 2 h at 200 °C under a constant nitrogen flow. Each analysis was

150   initiated by measuring the free space in the vial. The specific surface areas were derived

151   from 6 pressure-point measurements (relative pressure $p/p0 = 0.05\text{-}0.3$, equilibration time 5

152   s) with nitrogen as adsorbing gas (Brunauer et al., 1938). The instrumental error was 0.1-0.3

153   m^2 g^{-1}, which corresponds to a relative error of about 1 %. The performance of the instrument

154   was monitored with the surface area reference material Carbon Black (21.0 ± 0.75 m^2 g^{-1})

155   provided by Micromeritics.

156

157   2.4 X-Ray Fluorescence

158   The mineral composition of ~1 g freeze-dried, homogenized subsamples was characterized

159   with a wavelength dispersive sequential Philips PW2400 X-ray Fluorescence (XRF)

160   spectrometer. The XRF was operated under vacuum conditions on samples prepared as

161   glass beads using lithium tetraborate and melted with a fluxer Claisse Fluxy (~1150°C)

162   (Mercone et al., 2001). The relative error was less than 0.6 % for major elements and less

163   than 3 % for trace elements. In this study only SiO_2, Al_2O_3 and CaO are reported.

164

165   2.5 Bulk elemental and carbon isotope analysis

166   Total organic carbon (TOC) concentrations and $\delta^{13}C$ isotopic composition were determined

167   at the Stable Isotope Laboratory, Department of Geological Sciences, Stockholm University.

168   Homogenized subsamples of ~10 mg were repeatedly acidified (HCl,1.5 M, Ag capsules) to

169   remove carbonates (Nieuwenhuize et al., 1994). TOC concentrations and $\delta^{13}C$ isotopic

170   composition were measured simultaneously with a Carlo Erba NC2500 elemental analyzer

171   connected via a split interface to a Finnigan MAT Delta V mass spectrometer. TOC

172   concentrations were blank corrected and the relative error was < 1 %. Stable isotope data

173   are reported relative to VPDB using the $\delta^{13}C$ notation.

174   Radiocarbon analyses of acidified samples were conducted at the US National Ocean

175   Sciences Accelerator Mass Spectrometry (NOSAMS) Facility of the Woods Hole

176   Oceanographic Institution, USA, according to their standard routines (Pearson et al., 1998).

177   The relative error of the measurements was < 0.5 %. Radiocarbon data are reported using

178   the $\Delta^{14}C$ notation following Stuvier and Polach (1977).

179

180   2.6 Biomarkers

181   2.6.1 CuO-oxidation products

182   Microwave-assisted alkaline CuO oxidation was performed according to the method

183   established by Goñi and Montgomery (2000). Homogenized subsamples of 100-400 mg of

184   sediment (corresponding to 2-5 mg OC) were combined with 300 mg of copper(II) oxide and

185   50 mg of ferrous ammonium sulfate and oxidized under oxygen-free conditions (degassed

186   NaOH, 8 wt %) at 150 °C for 90 min using an UltraWAVE Milestone 215 Microwave. After

187   oxidation, known amounts of trans-cinnamic acid and ethyl vanillin were added as recovery

188   standards. Samples were acidified to pH 1 with HCl (12 M) and repeatedly extracted with

189   ethyl acetate. Anhydrous Na_2SO_4 was added to remove remaining water. The solvent was

Biogeosciences

Open Access

EGU

Discussions

190 evaporated and extracts re-dissolved in pyridine. For quantification, subsamples were

191 derivatized with bis-trimethylsilyl-trifluoroacetamide (BSTFA) + 1 % trimethylchlorosilane

192 (TMCS) and analyzed on a gas-chromatograph mass spectrometer in full scan mode (GC-

193 MS, Agilent) using a DB5-MS capillary column (60 m x 250 µm, 0.25 µm stationary phase

194 thickness, Agilent J&W) with a temperature profile of initially 60 °C followed by a ramp of 5

195 °C min^{-1} until reaching and holding 300 °C for 5 min. The quantification of lignin phenols,

196 benzoic acids, and p-hydroxybenzenes was achieved by comparison to the response factors

197 (key ions) of commercially available standards. For cutin-derived products, fatty acids and

198 dicarboxylic acids the response factor of trans-cinnamic acid was used as in Goñi et al.

199 (1998).

200

201 2.6.2 Solvent-extractable Lipids

202 Wax lipids were extracted by means of accelerated solvent extraction (Dionex ASE 300)

203 using dichloromethane:methanol (9:1) according to the method described by Wiesenberg et

204 al. (2004). Pre-rinsed stainless-steel vessels were loaded with ~3 g of freeze-dried sediment,

205 filled up with pre-combusted glass beads and pre-combusted glass fiber filters at both ends.

206 Two extraction cycles were performed per sample applying a static pressure of 1500 psi and

207 a temperature of 80 °C for 5 min after a heating phase of 5 min. The flush volume was 50 %

208 of the 34 ml cell size with a purging time of 100 s.

209 Extracts were further cleaned (addition of activated Cu for sulfur and anhydrous Na_2SO_4 for

210 water removal) and then separated into a neutral and an acid fraction using BondElut

211 cartridges (bonded phase NH_2, Varian), eluting with dichloromethane:isopropanol (2:1) for

212 the neutral and methyl *tert*-butyl ether with 4 % acetic acid for the acid fraction according to

213 the method described by van Dongen et al. (2008a). The neutral fraction was further

214 separated into a polar and a non-polar fraction with an Al_2O_3 column. For each of the three

215 compound classes *n*-alkanes (neutral non-polar fraction), *n*-alkanols (neutral polar fraction)

216 and *n*-alkanoic acids (acid fraction) ~10 mg of one internal standard, d_{50}-tetracosane, 2-

217 hexadecanol and d_{39}-eicosanoic acid respectively, were added to the sediment samples prior

218   to extraction. All fractions were then analyzed on a GC–MS (Agilent) using the same column

219   and temperature program as for the CuO products. The polar and acid fractions were

220   derivatized with BSTFA + 1 % TMCS prior to analysis. Quantification was performed using a

221   5-point calibration curve with commercially available standards.

3   Results and Discussion

The fate of permafrost-released terrigenous organic carbon (TerrOC) across the Laptev Sea

shelf is controlled by competing processes. Degradation and sorting, as well as replacement

of TerrOC by autochthonous marine organic matter all co-occur to varying degrees during

cross-shelf transport. To disentangle their effects on the fate of permafrost-released TerrOC

we first report changes in bulk sediment and OC properties and then focus on differences on

the molecular level.

3.1 Characterization of the transect on a bulk level

Bulk total organic carbon (TOC) concentrations decreased across the shelf with highest

values (~2 %) at shallow water depths and lowest values on the shelf edge (~0.8 %); at high

water depths (> 2000 m) concentrations were slightly higher (~1 %). TOC values and the

general pattern were in accordance with previous data from the Laptev Sea (Semiletov et al.,

2005; Shakhova et al., 2015; Stein and Fahl, 2004; Vonk et al., 2012) and within the same

range of those measured for the North American Arctic margin (Goni et al., 2013).

Normalizing TOC concentrations to the mineral-specific surface area (SA) helps to

understand the influence of physical sorting and preferential deposition on the observed TOC

trends since SA is correlated to the sediment grain size to a first order approximation. To test

if the mineral surface area is altered by the input of autochthonous organisms with siliceous

or carbonaceous skeleton (e.g. silicoflagellates/diatoms or foraminifera/shells respectively),

the mineral composition of the sediments was examined by X-ray fluorescence analysis.

There were no apparent trends with water depth for either SiO_2/Al_2O_3 or CaO/Al_2O_3;

therefore, marine production is not expected to have a measureable effect and SA can thus

be regarded as a conservative parameter. This was also confirmed by low biogenic silica

concentrations for the Laptev Sea reported earlier (< 1.4 %, Mammone, 1998).

The relationship between TOC and SA has been widely studied on continental margins (e.g.

Blair and Aller, 2012; Keil et al., 1994; Mayer, 1994). The TOC/SA ratios of typical river

suspended sediments range between 0.4 and 1 mg m^{-2}. TOC/SA ratios > 1 mg m^{-2} have

250   been found in areas with high TOC supply (e.g. river outlets) and where the deposited

251   organic matter had spent little time under oxic conditions (short oxygen exposure time, OET).

252   Ratios < 0.4 mg m^{-2} generally correspond to sediments from deeper parts of the ocean and

253   long OETs. Accordingly, the TOC/SA values along the Laptev Sea transect displayed a

254   strong decrease from 2.2 and 1.7 mg m^{-2} close to the Lena River delta (water depths of 11

255   and 7 m, respectively) to about 0.3 mg m^{-2} at water depths greater than 2000 m (Fig. 2A),

256   proposing extensive TOC loss during cross-shelf transport.

257   Bulk TOC isotopes have been broadly used to distinguish between organic matter sources.

258   Radiocarbon isotopes (^{14}C) convey information about the age of organic material, with

259   younger OC having higher Δ^{14}C values. Marine organic matter produced primarily from CO_2

260   is expected to have modern ^{14}C signatures, whereas permafrost-derived TerrOC has aged

261   both on land and during transport and has thus more depleted ^{14}C values. The Δ^{14}C values

262   for our Laptev Sea transect were generally low (< -280 ‰, Fig. 2B), suggesting a significant

263   input of pre-aged TerrOC (as in Vonk et al., 2012). Bulk TOC showed less depleted Δ^{14}C

264   signatures with increasing distance from land on the shelf (from about -500 ‰ to about -340

265   ‰ on the outer shelf, Fig. 2B), reflecting a dilution of older TerrOC with younger marine

266   material. On the slope and rise, however, Δ^{14}C values decreased again to about -410 ‰.

267   This difference may be a result of ageing during lateral transport and/or after deposition due

268   to lower accumulation rates on slope and rise. The range between -340 ‰ and -410 ‰

269   corresponds to a Δ^{14}C age difference of about 900 years; however, the depositional age

270   differences between shelf and slope samples were estimated to be less than 80 years (see

271   Section 2.2). Ageing after burial alone does therefore not explain the difference in Δ^{14}C. Keil

272   et al. (2004) estimated a lateral transport time of 1800 years across the Washington margin

273   (158 km) from Δ^{14}C data of bulk OC in surface sediments. For the > 200 km distance

274   between mid-shelf and rise a bulk ageing of 900 years does therefore not seem

275   unreasonable. It has to be taken into account, however, that mainly the TerrOC fraction of

276   the bulk OC is subject to such protracted lateral transport. Transport times would thus have

277   to be significantly higher in order to explain this age difference for the entire bulk OC.

278   For stable carbon isotopes (^{13}C), terrigenous sources are generally more depleted than

279   marine organic matter (Fry and Sherr, 1984). In this study, values for δ^{13}C of TOC ranged

280   between -26.5 ‰ and -22.3 ‰. The trend towards more enriched TOC with increasing

281   distance from the coast (Fig. 2B) can be explained by a growing proportion of marine organic

282   matter. However, the δ^{13}C signature of the marine source appeared to be heavier than typical

283   marine planktonic material in that region (-26.7 ± 1.2 ‰, Panova et al., 2015; -24 ± 3 ‰,

284   Vonk et al., 2012, and citations therein). One possible explanation for this discrepancy is an

285   underestimated influence of ice algae that were reported to have highly enriched δ^{13}C values

286   between -15 to -18 ‰ (Schubert and Calvert, 2001). Significant seafloor deposition of ice

287   algal biomass has been observed previously for the Arctic basins (Boetius et al., 2013).

288   Another option would be a more refractory, isotopically-enriched marine endmember (-21.2

289   ‰) as suggested by Magen et al. (2010). They argue that lighter isotopes are preferentially

290   consumed by bacteria, which in turn enriches the remaining marine organic matter. Following

291   their reasoning, the more enriched values observed for this transect may be interpreted as a

292   increasing proportion of refractory marine organic matter.

293   Winterfeld et al. (2015b) analyzed surface water particulate organic carbon (POC) in the

294   Lena River delta and found a mean δ^{13}C of -29.6 ± 1.5 ‰. Karlsson et al. (2011) reported

295   similarly depleted δ^{13}C values for POC from the Buor-Khaya Bay (-29.0 ± 2.0 ‰), while their

296   mean value for sedimentary OC for the same stations was significantly more enriched (-25.9

297   ± 0.4 ‰) and agreed well with our data for the shallow stations (-26.2 ± 0.3 ‰, stations YS-

298   13, YS-14 and TB-46). Lena River POC δ^{13}C values from high-discharge periods agree well

299   with the more enriched values we found for the shallow stations (Rachold and Hubberten,

300   1998). Stein and Fahl (2004), Semiletov et al. (2011, 2012) and Vonk et al. (2012) presented

301   similar δ^{13}C ranges and trends for sediments from parts of the Laptev Sea as is reported in

302   the current study for the entire width of the Laptev Sea shelf. For the Arctic Amerasian

303   Continental shelf, Naidu et al. (2000) reported contrasts in absolute δ^{13}C values comparing

304   surface sediment samples from different regions, but all commonly displayed an increasing

305   trend for $\delta^{13}C$ values across the shelf, suggesting a growing fraction of marine organic matter

306   with increasing distance from the coast.

307   Combining TOC/SA ratios with stable isotope signatures ($\delta^{13}C$) may serve to disentangle two

308   different processes, which occur synchronously during cross-shelf transport (as in Keil et al.

309   1997a): 1.) The net loss of TerrOC and 2.) the replacement of TerrOC with autochthonous

310   marine OC.

311   Net loss of TerrOC, caused by either degradation or hydrodynamic sorting during transport,

312   has been quantified previously using TOC/SA ratios (Aller and Blair, 2006; Keil et al., 1997a).

313   The carrying-capacity of inorganic particles for OC is assumed to be a function of the SA

314   (Mayer, 1994); a decrease in TOC/SA values can therefore be regarded as TOC net loss.

315   Replacement of TerrOC with autochthonous marine OC does not change this ratio. But since

316   marine OC is known to be isotopically enriched in $\delta^{13}C$ over TerrOC, this process is recorded

317   by an increasing isotopic signature. Along the Laptev Sea transect, both processes seemed

318   to play an important role (Fig. 2C). High TOC/SA values close to the Lena River decreased

319   sharply, pointing to extensive net loss, while the increase in $\delta^{13}C$ values was minor in this

320   area. Once TOC/SA ratios were < 0.8 mg m^{-2} (water depths > 20 m), the isotopic changes

321   and thus the replacement of TerrOC with marine OC became increasingly important. Similar

322   trends were observed for the Amazon River delta (Keil et al., 1997b).

323   However, the TOC/SA trend in the shallower sediments is likely driven by both degradation

324   of OC bound to the mineral matrix during cross-shelf transport and sorting of vascular plant

325   fragments that are retained in the inner-shelf. A recent study (Tesi et al., 2016) has shown

326   that ~50 % of the total OC pool in the inner Laptev shelf surface sediments exists in the form

327   of large vascular plant fragments. They are trapped close to the coast due to their size

328   (Stoke's law), while the OC bound to the fine mineral matrix is more buoyant and transported

329   offshore towards deeper waters.

330

331   3.2 Molecular indicators of organic matter sources

332   3.2.1   Biomarker distributions

333   The abundances of different source-diagnostic molecular proxies have been extensively

334   investigated to elucidate complex carbon-cycling mechanisms. In this study, a biomarker

335   suite of CuO oxidation products and solvent-extractable lipids was analyzed in order to gain

336   more insights on TerrOC sources and degradation status along the Laptev Sea transect. All

337   biomarker concentrations were normalized to the sediment-specific surface area (SA)

338   instead of OC content to avoid the signals being overshadowed by other carbon pools. As

339   shown by the lack of water depth related changes in the mineral composition (Section 3.1),

340   mineral-matrix dilution by biogenic material is negligible.

341   Lignin-derived phenols have been widely used to trace TerrOC in the marine environment

342   (e.g. Ertel and Hedges, 1984; Goñi and Hedges, 1995; Hedges and Mann, 1979). The lignin

343   macro-molecule is only synthesized in vascular plants (and certain seaweed species that are

344   not existent in the study area) to render stability to the cell walls. Across the shelf, lignin

345   loadings decreased substantially with increasing distance from the coast/water depth (45 µg

346   m^{-2} close to the coast, 0.43 ± 0.09 µg m^{-2} for the deep stations; loss of 99.1 ± 0.2 %, Fig. 3A).

347   Cutin-derived hydroxy fatty acids are another compound class obtained from CuO oxidation,

348   which have been used in parallel with lignin phenols (e.g. Goñi et al., 2000; Prahl et al.,

349   1994). They are mainly associated with the soft tissues of vascular plants such as leaves and

350   needles. Cutin acid loadings displayed a similar trend as lignin phenols (11 µg m^{-2} close to

351   the coast, 0.061 ± 0.010 µg m^{-2} for the deep stations; loss of 99.4 ± 0.1 %, Fig 3A).

352   Similar values and sharp declines with increasing distance from the coast for lignin and cutin

353   have been observed for the whole East Siberian Arctic Shelf (ESAS) (Tesi et al., 2014). A

354   recent study (Winterfeld et al., 2015a) for the Buor-Khaya Bay (5.8-17 m water depth)

355   reported lignin phenol concentrations on the same order of magnitude, up to 40 % higher for

356   the shallowest samples, and decreasing with increasing depth. For the Beaufort Sea shelf,

357   Goñi et al. (2000) found a less drastic decline in lignin phenols and cutin acids going from 5

358   m water depth to 210 m, which likely reflected both lower concentrations in the shallow

359   waters (factor of ~2), and a narrower and steeper shelf. Lignin phenols were also higher at

360   greater water depths than on the ESAS. This may reflect the differences in bathymetry: since

Biogeosciences
Discussions

EGU
Open Access

361   the Beaufort Sea shelf is not as wide as, but steeper than the ESAS, lateral transport is

362   possibly faster, leaving less time for organic matter to be degraded along the way. A

363   comparison between different shelf-slope systems across the North American Arctic margin

364   (Goni et al., 2013) revealed very low lignin and cutin concentrations for the Canadian

365   Archipelago, Lancaster Sound and Davis Strait, whereas both concentrations and trends with

366   water depth for the Beaufort Sea, Chuckchi Sea and Bering Sea were similar to the results

367   from this study. An exception to these patterns was Barrow Canyon, where at water depths

368   of > 2000 m lignin and cutin concentrations were as high as the ones observed close to the

369   Lena River delta, pointing to efficient rapid TerrOC transfer with comparably short oxygen

370   exposure times through this active canyon (Goni et al., 2013).

371   Solvent extractable high-molecular weight (HMW) *n*-alkanes and *n*-alkanoic acids make up

372   the major part of epicuticular leaf waxes (Eglinton and Hamilton, 1967) and have been

373   broadly employed as TerrOC biomarkers (for the Arctic Ocean e.g. van Dongen et al., 2008;

374   Yunker et al., 1995, 2005). HMW wax lipids in this study also presented a decreasing trend

375   with increasing water depth/distance from the coast, but to a lesser extent than lignin phenols

376   or cutin acids (HMW *n*-alkanes, carbon chain-lengths of 23-34: 1.1 µg m^{-2} close to the coast,

377   0.12 ± 0.02 µg m^{-2} for the deep stations; HMW *n*-alkanoic acids, chain-lengths 24-30: 12 µg

378   m^{-2} close to the coast, 0.42 ± 0.29 µg m^{-2} for the deep stations; loss of 89 ± 2 % and 96 ± 3

379   %, respectively).

380   Previous studies in the same area reported similar lipid biomarkers concentrations, which

381   confirm the magnitude of the decreasing trends with increasing water depth (Karlsson et al.,

382   2011; Vonk et al., 2010). HMW *n*-alkane concentrations in the Beaufort and the Chuckchi

383   Sea (Belicka et al., 2004; Yunker et al., 1993) are in accordance with the ones measured on

384   the ESAS, but the shallowest sample on the Beaufort Shelf is ~2 times lower than the

385   shallow ESAS samples. This might imply that sediments transported by the Mackenzie River

386   to the Beaufort Shelf have lower TerrOC concentrations than Lena River transported

387   sediments. For the Mackenzie Shelf Goñi et al. (2000) used lignin phenols and cutin acids to

388   estimate a marine δ^{13}C endmember and therewith derived a terrigenous contribution of

389 almost 80 % for the shallowest sediments, while rough estimates from C/N and $\delta^{13}C$ data

390 suggested that TerrOC made up only 30-50 % of the organic carbon (Macdonald et al.,

391 2004). For the Lena Delta, source apportionment calculations using $\delta^{13}C$ and $\Delta^{14}C$ data

392 attributed up to 83 % of the organic carbon to terrigenous sources (Vonk et al., 2012).

393 All TerrOC biomarker loadings displayed a strong decrease across the shelf, but their relative

394 losses differ substantially between compound classes (Fig. 3C). These findings agree with

395 previous results for the ESAS (Tesi et al., 2014), where similar differences between

396 biomarkers were reported. A larger decrease was observed for lignin than for cutin, in

397 contrast to this study. The different extents of biomarker losses for the different compound

398 classes may either be attributed to preferential degradation of lignin phenols and cutin acids,

399 implying that they are more labile than HMW *n*-alkanes and *n*-alkanoic acids, or sorting

400 during transport, suggesting that they are associated with a sediment fraction that is

401 hydraulically retained and carried less efficiently to the outer shelf/slope. A recent study (Tesi

402 et al., 2016) aimed to disentangle these two processes by analyzing different fractions of bulk

403 surface sediments from three transects (with three stations each) on the ESAS. The fractions

404 were separated according to density (1.8 g cm^{-3} cutoff), size (>63 µm, 38-63 µm, < 38 µm)

405 and settling velocity (1 m d^{-1} cutoff). The highest lignin phenol abundance was found in low-

406 density plant fragments (26-55 mg g^{-1} OC). These large particles have a higher settling

407 velocity (Stokes' law) and are therefore hydraulically retained close to the coast. Cutin acids

408 and plant wax lipids were mainly associated with the mineral high-density fine (< 38 µm, > 1

409 m d^{-1}) and ultrafine (< 38 µm, < 1 m d^{-1}) fractions. Within the fine and ultrafine fractions,

410 which made up about 95 % of the organic carbon on the outer shelf, they found drastic

411 losses of all biomarkers with increasing distance from the coast, which they attributed to

412 degradation during the protracted cross-shelf transport. Relative decreases appeared to

413 depend on the number of functional groups of the compound class: 98 ± 1 % for lignin

414 phenols, 97 ± 1 % for cutin acids, 96 ± 1 % for HMW *n*-alkanoic acids and 89 ± 4 % for HMW

415 *n*-alkanes. According to that study, the steep cross-shelf gradients observed here for lignin

416 phenols can be attributed to both hydrodynamic sorting close to the coast and degradation

Biogeosciences
Discussions

Open Access

EGU

417 during transport. The other compounds analyzed are mainly affected by degradation and

418 experience sorting to a lesser extent.

419 Degradation after burial is assumed to play only a minor role in this study. Differences in

420 sedimentation ages are expected to be small (Section 2.1) and a study on centennial-scale

421 sediment cores from the East Siberian Sea (Bröder et al., 2016) detected no significant

422 TerrOC degradation (as recorded by biomarker loss) with increasing sediment depth. Also in

423 that study, lignin phenol and cutin acid loadings were on average 20 times higher on the

424 inner than on the outer shelf, whereas for HMW n-alkanoic acids and n-alkanes the

425 difference between inner and outer shelf was only a factor of ~3-5. Contrasts between the

426 stations were found to be larger than down-core changes. This may be due to the fact that

427 the cores in that study only encompassed about one century of sedimentation ages, while

428 the protracted cross-shelf transport possibly requires much longer timescales.

429

430 3.2.2 Lignin Phenol sources

431 Relative distributions of different lignin phenol classes reveal more TerrOC source

432 information since they are specific to different plant types. Syringyl phenols are not produced

433 by gymnosperm (non-flowering) plants; elevated syringyl to vanillyl ratios (i.e. S/V > 1,

434 Hedges and Parker, 1976) are therefore attributed to more lignin phenols from angiosperm

435 (flowering) plants. These ratios have to be handled with care, though, because the

436 preferential degradation of syringyl phenols by white- and brown-rot fungi on land can also

437 alter S/V ratios (Hedges et al., 1988). S/V values for the Laptev Sea transect increased with

438 increasing water depth from ~0.65 for the inner shelf to ~1.0 for the slope/rise sediments

439 (Fig. 5A). This trend can either be explained by preferential degradation of gymnosperm

440 material or sorting during transport. Tesi et al. (2014) measured generally lower values for

441 S/V (ESAS average: 0.47, for only Lena watershed dominated locations: 0.42) recording no

442 trend with water depth. Their deepest station was located at only 69 m water depth, though,

443 whereas in this study sediments from down to 3146 m water depth were analyzed. S/V ratios

444 in Buor-Khaya Bay surface sediments (Winterfeld et al., 2015a) were also lower (0.43 ± 0.02

445   on average) and displayed no trend with water depth. Within the water depth interval they

446   studied (5.8-17 m), however, the samples analyzed in this study had also quite

447   homogeneous S/V ratios (0.64 ± 0.02). Two sediment cores from the East Siberian Sea

448   (Bröder et al., 2016) showed also lower S/V values (inner shelf surface sediment: 0.62, outer

449   shelf surface sediment: 0.50) displaying no clear trends over time/down-core. For the

450   Beaufort Sea shelf Goñi et al. (2000) detected rather high values (0.54-1.71), which (besides

451   the very high value at 61 m water depth) agree with the data from this study. Other transects

452   across the North American Arctic margin (Goni et al., 2013) had slightly lower S/V ratios with

453   no observed trends with water depth.

454   The ratio of cinnamyl to vanillyl phenols (C/V) is associated with the relative contributions of

455   woody versus soft material, because only non-woody vascular plants synthesize cinnamyl

456   phenols (Hedges and Mann, 1979a). This ratio admittedly decreases with ongoing

457   degradation (Opsahl and Benner, 1995) and may therefore not be used as an unambiguous

458   source indicator. We observed that C/V values strongly decreased across the Laptev Sea

459   Shelf from ~0.5 (close to the Lena River outlet) to ~0.1 (on the slope/rise, Fig. 5B), which

460   may reflect the preferential degradation of soft tissues. This trend is not likely caused by

461   hydrodynamic sorting, since typically the larger, low-density, woody plant fragments are

462   retained in shallower water, whereas finer material is transported further across the shelf

463   (e.g. Keil et al., 1994; Tesi et al., 2016).

464   C/V ratios in Buor-Khaya Bay sediments (Winterfeld et al., 2015a) in shallow waters were on

465   average lower and more homogeneous (0.17 ± 0.03) than those measured in this study (0.41

466   ± 0.12 for the corresponding depth interval). C/V values for the entire ESAS were on average

467   0.15 (0.14 ± 0.07 for only Lena dominated waters) with no water depth trend (Tesi et al.,

468   2014). In shallow sediment cores from the East Siberian Sea, Bröder et al. (2016) measured

469   C/V ratios of 0.20 (inner shelf) and 0.13 (outer shelf) for the surface sediments with no

470   significant trend over sediment depth. For the Mackenzie Shelf C/V values ranged between

471   0.16 and 0.32 and slightly increased with increasing water depth (Goñi et al., 2000). In

472   contrast, in the Bering Sea, Chuckchi Sea, Barrow Canyon, Canadian Archipelago,

473   Lancaster sound and Davis Strait there were no C/V trends observed (Goni et al., 2013), with

474   lower values in the Canadian part (0.10 ± 0.12) and highest values on the Beaufort Sea

475   slope, where values slightly decreased with increasing depth (0.39 ± 0.07).

476   A comparison to the S/V-C/V signatures of potential Arctic plant end-members (compiled by

477   Amon et al., 2012, and citations therein, Tesi et al., 2014, and Winterfeld et al., 2015a)

478   showed that lignin phenols likely derive from both angio- and gymnosperm soft tissues in the

479   shallower samples, closely matching with willow (*Salix*) tissues measured by Winterfeld et al.

480   (2015a). With increasing water depths, angiosperm wood became the most important source

481   material, while gymnosperm wood, grasses and mosses did not appear to contribute

482   significantly to the overall lignin phenol fingerprint (Fig. 5C). As discussed earlier, this trend

483   may well be a result of preferential degradation and sorting during cross-shelf transport and

484   not derive from actual changes in source material.

485

486   3.3 Degradation status of organic matter

487   During degradation, syringyl and vanillyl phenol aldehydes are oxidized to carboxylic acids of

488   the same phenol group. Increasing Sd/Sl and Vd/Vl ratios can therefore qualitatively indicate

489   ongoing degradation of lignin phenols (Ertel and Hedges, 1984; Hedges et al., 1988). For

490   fresh plant material typical acid-to-aldehyde ratios are around 0.1-0.2 (Hedges et al., 1988).

491   Winterfeld et al. (2015a), however, found values as high as Sd/Sl = 0.80 and Vd/Vl = 0.67 for

492   a moss species (*Aulacomnium turgidum*), Sd/Sl = 0.87 for larch (*Larix*) needles and Sd/Sl =

493   0.49 Vd/Vl = 0.41 for wild rosemary (*Ledum palustre*). Sedges (*Carex spp.*), dwarf birch

494   (*Betula nana*) and willow (*Salix*) range between Sd/Sl = 0.13-0.24 and Vd/Vl = 0.18-0.23.

495   The ratio of CuO oxidation-derived 3,5-dihydroxybenzoic acid to vanillyl phenols (3,5-Bd/V)

496   also serves as a proxy for degradation as 3,5-Bd is formed during humification likely

497   occurring in soils (Gordon and Goñi, 2004; Hedges et al., 1988; Prahl et al., 1994; Tesi et al.,

498   2014). For this reason, this proxy can trace mineral rich soil organic matter in contrast to

499   vascular plant debris (e.g. Dickens et al., 2007; Prahl et al., 1994) as well as degradation

500   during cross shelf transport (Tesi et al., 2016).

501   Sd/Sl, Vd/Vl and 3,5-Bd/V all increased along the transect, implying more degraded material

502   with increasing residence time in the shelf system. There appeared to be no differences

503   between outer shelf/slope and rise, which may indicate that TerrOC on the slope is already

504   highly reworked. In contrast, Tesi et al. (2014) found no correlation between Sd/Sl or Vd/Vl

505   and distance from the coast, while 3,5-Bd/V significantly increased with increasing distance

506   from the coast. Sd/Sl values for the Buor-Khaya Bay from Winterfeld et al. (2015a) were

507   slightly higher (1.04 ± 0.24) than samples from the corresponding water depths in this study

508   (0.66 ± 0.15), whereas Vd/Vl values were significantly higher (1.28 ± 0.30 compared to 0.59

509   ± 0.14). Measurements for the Mackenzie Shelf agreed with the ones in this study (Sd/Sl =

510   0.81 ± 0.25 compared to 1.01 ± 0.33 for the corresponding water depths; Vd/Vl = 0.69 ± 0.14

511   to 0.86 ± 0.26; 3,5-Bd/V = 0.19 ± 0.04 to 0.31 ± 0.15), but did not show a trend with water

512   depth (Goñi et al., 2000).

513   Tesi et al. (2016) found no difference in acid/aldehyde ratios between different density, grain

514   size or settling velocity fractions of surface sediments from three (shorter) transects on the

515   ESAS; it can thus be assumed that these proxies are not affected by hydrodynamic sorting

516   during transport. Degradation-caused changes were limited to the lignin-rich low-density

517   fraction, where Vd/Vl and Sd/Sl increased with increasing distance from the coast. Bulk 3,5-

518   Bd/V values are potentially affected by both sorting and degradation, as they increased with

519   decreasing particle size (fine and ultrafine fractions had the most degraded signal and are

520   preferentially transported to the outer shelf) and across the shelf in each of the fractions.

521   The carbon preference indices for HMW *n*-alkanes and HMW *n*-alkanoic acids have also

522   been widely applied as degradation proxies for plant waxes in marine sediments (for the

523   ESAS, e.g. van Dongen et al., 2008; Fahl and Stein, 1997; Fernandes and Sicre, 2000; Vonk

524   et al., 2010). It measures the ratio of odd-to-even numbers of carbon chain-lengths of HMW

525   lipids and is based on the preference of odd carbon chain-lengths for HMW *n*-alkanes in

526   fresh plant material (even carbon chain-lengths for HMW *n*-alkanoic acids; Eglinton and

527   Hamilton, 1967). With ongoing degradation this preference is lost and the CPI approaches 1

528   (Bray and Evans, 1961).

529   We observed that the HMW *n*-alkane CPI presented the same pattern as the lignin phenol

530   based degradation indices, however, the HMW *n*-alkanoic acid CPI did not show as much of

531   a degradation trend (HMW *n*-alkane CPI: ~5.7 close to the coast, ~2.2 for the deep stations;

532   HMW *n*-alkanoic acids: ~5.4 close to the coast, ~4.1 for the deep stations). Karlsson et al.

533   (2011) measured lipid CPIs in the Buor-Khaya Bay with 10-80 km distance to the coast and

534   obtained similar results to this ~800 km cross-shelf study, with higher values closer to the

535   river delta. Their data appears to have a wider spread, though, which might be due to either

536   the narrower dynamics range, or a different definition of high- molecular weight: in this study,

537   carbon chain lengths of ≥ 23 for *n*-alkanes and ≥ 24 for *n*-alkanoic acids were defined as

538   HMW, whereas Karlsson et al. (2011) used ≥ 21 for both compound classes. Fahl and Stein

539   (1997) also reported a large range of *n*-alkane CPI values (< 0.2- > 5) for Laptev Sea

540   sediments. Fernandes and Sicre (2000) analyzed sediments from the Kara Sea and from the

541   major rivers discharging into this sea, Ob and Yenisey rivers. In the marine environment and

542   the Ob River, they observed HMW *n*-alkane CPI values between 4.8 and 5.3, similar to those

543   found at shallow water depths in this study. For the Yenisey River and mixing zone, they

544   found higher CPI values, pointing to fresher material being transported there. Vonk et al.

545   (2010) recorded HMW *n*-alkane CPI values for sediments along the East Siberian Sea

546   Kolyma paleoriver transect (across the East Siberian Sea) shelf that decreased from > 7.5 to

547   < 4.0 with increasing distance from the river mouth, overall higher than in this study but

548   confirming the general trend to more degraded material on the outer shelf. Tesi et al. (2016)

549   found HMW *n*-alkanoic acid CPI values to decrease with decreasing particle size with no

550   significant trends across the shelf in all but the low-density fraction, which is largely retained

551   close to the shore. The HMW *n*-alkane CPI values in that study, however, showed no

552   systematical differences between different fractions, but an overall decreasing trend with

553   increasing distance from the coast.

554   When undergoing degradation, HMW *n*-alkanoic acids may also lose their functional groups,

555   turning them into HMW *n*-alkanes (Meyers and Ishiwatari, 1993). The slightly decreasing

556   ratio of HMW *n*-alkanoic acids to *n*-alkanes also hints at more degraded material with

22

557 increasing water depth, although, due to a rather large variability, this trend is not significant.

558 For the Buor-Khaya Bay surface sediments Karlsson et al. (2011) obtained similar results

559 (0.48-10.7, here 1.1-10.9) with higher values closer to the river delta. Along the Kolyma

560 paleoriver transect, Vonk et al. (2010) measured HMW n-alkanoic acid to n-alkane ratios

561 between 1 and 6 with no clear trend with increasing distance from the river mouth. Tesi et al.

562 (2016) found decreasing values with increasing distance from the coast with no differences

563 between the fractions. Two sediment cores from inner and outer East Siberian Sea recording

564 about one century of sedimentation showed no clear trend in CPI or HMW n-alkanoic acid/n-

565 alkane towards more degraded TerrOC with increasing sediment depth (Bröder et al., 2016),

566 but displayed a similar difference between inner and outer shelf as seen in this study. This

567 contrasting behavior for cross-shelf and down-core trends may be caused by significantly

568 different timescales for the two processes: about one century in situ/after burial compared to

569 potentially several millennia long lateral transport. Furthermore, the degradation efficiency is

570 possibly higher under the oxic conditions prevailing during cross-shelf lateral transport (Keil

571 et al., 2004), than in the anoxic conditions that predominate below a few millimeters of

572 sediments on the ESAS (e.g. Boetius and Damm, 1998). Comparing in situ to transport-

573 related oxygen exposure times on the wide Arctic shelves could potentially resolve the

574 observed discrepancies.

Biogeosciences

Discussions

Open Access

EGU

4 Concluding remarks and future research directions

Across the Laptev Sea from the Lena River mouth to the deep sea of the Arctic interior a

considerable loss of terrigenous organic matter has been observed on both bulk and

molecular level. All terrigenous biomarkers display a massive decline with increasing water

depth along this high-resolution transect due to hydrodynamic sorting and degradation during

transport. Terrigenous organic matter (TerrOC) seems to be also qualitatively more degraded

on the outer shelf, slope and rise compared to inner shelf and coastal areas.

These results corroborate and expand previous findings for the East Siberian Arctic Shelf,

showing that the shelf seas in this region function as an active reactor for TerrOC. This

stands in sharp contrast to e.g. the Mackenzie basin, which is thought to act as a geological

sink for organic carbon due to its efficient TerrOC burial (Hilton et al., 2015). For narrower

Arctic shelves in general, where transport times can be expected to be much shorter, organic

matter transfer towards the deeper basins appears to be much more efficient, with high

TerrOC concentrations in surface sediments even at greater water depths (e.g. Barrow

Canyon, Goni et al., 2013). It can therefore be assumed that the cross-shelf transport time

exerts first-order control over the extent of TerrOC degradation. With ongoing global

warming, rising permafrost-derived organic carbon input from river-sediment discharge and

coastal erosion is expected to reach the marine environment. It is therefore crucial to better

constrain cross-shelf transport times in order to determine a TerrOC degradation rate and

thereby contribute to quantifying potential carbon-climate feedbacks.

Biogeosciences

Discussions

EGU

Open Access

Biogeosciences
Discussions

Open Access

EGU

References

613

614 Aller, R. C. and Blair, N. E.: Carbon remineralization in the Amazon-Guianas tropical mobile mudbelt: A
615 sedimentary incinerator, Continental Shelf Research, 26(17-18), 2241–2259, doi:10.1016/j.csr.2006.07.016, 2006.

616 Amon, R. M. W., Rinehart, A. J., Duan, S., Louchouarn, P., Prokushkin, A., Guggenberger, G., Bauch, D.,
617 Stedmon, C., Raymond, P. A., Holmes, R. M., McClelland, J. W., Peterson, B. J., Walker, S. A. and Zhulidov, A.
618 V.: Dissolved organic matter sources in large Arctic rivers, Geochimica et Cosmochimica Acta, 94, 217–237,
619 doi:10.1016/j.gca.2012.07.015, 2012.

620 Belicka, L. L., Macdonald, R. W., Yunker, M. B. and Harvey, H. R.: The role of depositional regime on carbon
621 transport and preservation in Arctic Ocean sediments, Marine Chemistry, 86(1-2), 65–88,
622 doi:10.1016/j.marchem.2003.12.006, 2004.

623 Blair, N. E. and Aller, R. C.: The Fate of Terrestrial Organic Carbon in the Marine Environment, Annual Review of
624 Marine Science, 4(1), 401–423, doi:10.1146/annurev-marine-120709-142717, 2012.

625 Boetius, A. and Damm, E.: Benthic oxygen uptake, hydrolytic potentials and microbial biomass at the Arctic
626 continental slope, Deep-Sea Research Part I: Oceanographic Research Papers, 45(2-3), 239–275,
627 doi:10.1016/S0967-0637(97)00052-6, 1998.

628 Boetius, A., Albrecht, S., Bakker, K., Bienhold, C., Felden, J., Fernández-Méndez, M., Hendricks, S., Katlein, C.,
629 Lalande, C., Krumpen, T., Nicolaus, M., Peeken, I., Rabe, B., Rogacheva, A., Rybakova, E., Somavilla, R. and
630 Wenzhöfer, F.: Export of algal biomass from the melting Arctic sea ice., Science (New York, N.Y.), 339(6126),
631 1430–2, doi:10.1126/science.1231346, 2013.

632 Bray, E. . and Evans, E. .: Distribution of n-paraffins as a clue to recognition of source beds, Geochimica et
633 Cosmochimica Acta, 22(1), 2–15, doi:10.1016/0016-7037(61)90069-2, 1961.

634 Brunauer, S., Emmett, P. H. and Teller, E.: Adsorption of Gases in Multimolecular Layers, Journal of the
635 American Chemical Society, 60(2), 309–319, doi:citeulike-article-id:4074706\rdoi: 10.1021/ja01269a023, 1938.

636 Bröder, L., Tesi, T., Andersson, A., Eglinton, T. I., Semiletov, I. P., Dudarev, O. V., Roos, P. and Gustafsson, Ö.:
637 Historical records of organic matter supply and degradation status in the East Siberian Sea, Organic
638 Geochemistry, 91, 16–30, doi:10.1016/j.orggeochem.2015.10.008, 2016.

639 Charkin, A. N., Dudarev, O. V., Semiletov, I. P., Kruhmalev, A. V., Vonk, J. E., Sánchez-García, L., Karlsson, E.,
640 Gustafsson, O., Gustafsson, Ö. and Gustafsson, O.: Seasonal and interannual variability of sedimentation and
641 organic matter distribution in the Buor-Khaya Gulf: The primary recipient of input from Lena River and coastal
642 erosion in the southeast Laptev Sea, Biogeosciences, 8(9), 2581–2594, doi:10.5194/bg-8-2581-2011, 2011.

643 Dethleff, D.: Entrainment and export of Laptev Sea ice sediments, Siberian Arctic, Journal of Geophysical
644 Research C: Oceans, 110(7), 1–17, doi:10.1029/2004JC002740, 2005.

645 Dethleff, D.: Dense water formation in the Laptev Sea flaw lead, Journal of Geophysical Research: Oceans,
646 115(12), 1–16, doi:10.1029/2009JC006080, 2010.

647 Dickens, A. F., Gudeman, J. A., Gélinas, Y., Baldock, J. A., Tinner, W., Hu, F. S. and Hedges, J. I.: Sources and
648 distribution of CuO-derived benzene carboxylic acids in soils and sediments, Organic Geochemistry, 38(8), 1256–
649 1276, doi:10.1016/j.orggeochem.2007.04.004, 2007.

650 Dmitrenko, I. A., Kirillov, S. A. and Bruno Tremblay, L.: The long-term and interannual variability of summer fresh
651 water storage over the eastern Siberian shelf: Implication for climatic change, Journal of Geophysical Research:
652 Oceans, 113(3), 1–14, doi:10.1029/2007JC004304, 2008.

653 Eglinton, G. and Hamilton, R. J.: Leaf epicuticular waxes., Science (New York, N.Y.), 156(780), 1322–1335,
654 doi:10.1126/science.156.3780.1322, 1967.

655 Eicken, H., Reimnitz, E., Alexandrov, V., Martin, T., Kassens, H. and Viehoff, T.: Sea-ice processes in the Laptev
656 Sea and their importance for sediment export, Continental Shelf Research, 17(2), 205–233, doi:10.1016/S0278-
657 4343(96)00024-6, 1997.

658 Ertel, J. R. and Hedges, J. I.: The lignin component of humic substances: Distribution among soil and sedimentary
659 humic, fulvic, and base-insoluble fractions, Geochimica et Cosmochimica Acta, 48(10), 2065–2074,
660 doi:10.1016/0016-7037(84)90387-9, 1984.

661 Fahl, K. and Stein, R.: Modern organic carbon deposition in the Laptev Sea and the adjacent continental slope:

662   Surface water productivity vs. terrigenous input, Organic Geochemistry, 26(5-6), 379–390, doi:10.1016/S0146-
663   6380(97)00007-7, 1997.

664   Feng, X., Vonk, J. E., van Dongen, B. E., Gustafsson, Ö., Semiletov, I. P., Dudarev, O. V, Wang, Z., Montluçon,
665   D. B., Wacker, L. and Eglinton, T. I.: Differential mobilization of terrestrial carbon pools in Eurasian Arctic river
666   basins., Proceedings of the National Academy of Sciences of the United States of America, 110(35), 14168–73,
667   doi:10.1073/pnas.1307031110, 2013.

668   Feng, X., Gustafsson, Ö., Holmes, R. M., Vonk, J. E., van Dongen, B. E., Semiletov, I. P., Dudarev, O. V.,
669   Yunker, M. B., Macdonald, R. W., Montluçon, D. B. and Eglinton, T. I.: Multi-molecular tracers of terrestrial carbon
670   transfer across the pan-Arctic – Part 1: Comparison of hydrolysable components with plant wax lipids and lignin
671   phenols, Biogeosciences Discussions, 12(6), 4721–4767, doi:10.5194/bgd-12-4721-2015, 2015.

672   Fernandes, M. B. and Sicre, M. A.: The importance of terrestrial organic carbon inputs on Kara Sea shelves as
673   revealed by n-alkanes, OC and d13C values, in Organic Geochemistry, vol. 31, pp. 363–374., 2000.

674   Fry, B. and Sherr, E. B.: d13C Measurements as indicators of carbon flow in marine and freshwater ecosystems,
675   Contributions in Marine Science, 27, 13–49, 1984.

676   Goni, M. A., O'Connor, A. E., Kuzyk, Z. Z., Yunker, M. B., Gobeil, C. and Macdonald, R. W.: Distribution and
677   sources of organic matter in surface marine sediments across the North American Arctic margin, Journal of
678   Geophysical Research-Oceans, 118(9), 4017–4035, doi:10.1002/jgrc.20286, 2013.

679   Goñi, M. A. and Hedges, J. I.: Sources and reactivities of marine-derived organic matter in coastal sediments as
680   determined by alkaline CuO oxidation, Geochimica et Cosmochimica Acta, 59(14), 2965–2981, doi:10.1016/0016-
681   7037(95)00188-3, 1995.

682   Goñi, M. A. and Montgomery, S.: Alkaline CuO oxidation with a microwave digestion system: Lignin analyses of
683   geochemical samples, Analytical Chemistry, 72(14), 3116–3121, doi:10.1021/ac991316w, 2000.

684   Goñi, M. A., Ruttenberg, K. C. and Eglinton, T. I.: A reassessment of the sources and importance of land-derived
685   organic matter in surface sediments from the Gulf of Mexico, Geochimica et Cosmochimica Acta, 62(18), 3055–
686   3075, doi:10.1016/S0016-7037(98)00217-8, 1998.

687   Goñi, M. A., Yunker, M. B., MacDonald, R. W. and Eglinton, T. I.: Distribution and sources of organic biomarkers
688   in arctic sediments from the Mackenzie River and Beaufort Shelf, Marine Chemistry, 71(1-2), 23–51,
689   doi:10.1016/S0304-4203(00)00037-2, 2000.

690   Gordeev, V. V.: Fluvial sediment flux to the Arctic Ocean, Geomorphology, 80(1-2), 94–104,
691   doi:10.1016/j.geomorph.2005.09.008, 2006.

692   Gordon, E. S. and Goñi, M. A.: Controls on the distribution and accumulation of terrigenous organic matter in
693   sediments from the Mississippi and Atchafalaya river margin, Marine Chemistry, 92(1-4 SPEC. ISS.), 331–352,
694   doi:10.1016/j.marchem.2004.06.035, 2004.

695   Guay, C. K. H., Falkner, K. K., Muench, R. D., Mensch, M., Frank, M. and Bayer, R.: Wind-driven transport for
696   Eurasian Arctic rover discharge, Journal of Geophysical Research, 106(C6), 11469–11480, 2001.

697   Gustafsson, Ö., Van Dongen, B. E., Vonk, J. E., Dudarev, O. V. and Semiletov, I. P.: Widespread release of old
698   carbon across the Siberian Arctic echoed by its large rivers, Biogeosciences, 8(6), 1737–1743, doi:10.5194/bg-8-
699   1737-2011, 2011.

700   Günther, F., Overduin, P. P., Sandakov, A. V., Grosse, G. and Grigoriev, M. N.: Short- and long-term thermo-
701   erosion of ice-rich permafrost coasts in the Laptev Sea region, Biogeosciences, 10(6), 4297–4318,
702   doi:10.5194/bg-10-4297-2013, 2013.

703   Hedges, J. I. and Mann, D. C.: The characterization of plant tissues by their lignin oxidation products, Geochimica
704   et Cosmochimica Acta, 43(11), 1803–1807, doi:10.1016/0016-7037(79)90028-0, 1979a.

705   Hedges, J. I. and Mann, D. C.: The lignin geochemistry of marine sediments from the southern Washington coast,
706   Geochimica et Cosmochimica Acta, 43(11), 1809–1818, doi:10.1016/0016-7037(79)90029-2, 1979b.

707   Hedges, J. I. and Parker, P. L.: Land-derived organic matter in surface sediments from the Gulf of Mexico,
708   Geochimica et Cosmochimica Acta, 40, 1019–1029, 1976.

709   Hedges, J. I., Blanchette, R. A., Weliky, K. and Devol, A. H.: Effects of fungal degradation on the CuO oxidation
710   products of lignin: A controlled laboratory study, Geochimica et Cosmochimica Acta, 52(11), 2717–2726,
711   doi:10.1016/0016-7037(88)90040-3, 1988.

712   Hilton, R. G., Galy, V., Gaillardet, J., Dellinger, M., Bryant, C., O'Regan, M., Gröcke, D. R., Coxall, H., Bouchez, J.
713   and Calmels, D.: Erosion of organic carbon in the Arctic as a geological carbon dioxide sink, Nature, 524(7563),
714   84–87, doi:10.1038/nature14653, 2015.

715   Holmes, R. M., McClelland, J. W., Peterson, B. J., Shiklomanov, I. A., Shiklomanov, A. I., Zhulidov, A. V,
716   Gordeev, V. V and Bobrovitskaya, N. N.: A circumpolar perspective on fluvial sediment flux to the Arctic ocean,
717   Global Biogeochemical Cycles, 16(4), 14–45, doi:10.1029/2001GB001849, 2002.

718   Holmes, R. M., McClelland, J. W., Peterson, B. J., Tank, S. E., Bulygina, E., Eglinton, T. I., Gordeev, V. V.,
719   Gurtovaya, T. Y., Raymond, P. a., Repeta, D. J., Staples, R., Striegl, R. G., Zhulidov, A. V. and Zimov, S. a.:
720   Seasonal and Annual Fluxes of Nutrients and Organic Matter from Large Rivers to the Arctic Ocean and
721   Surrounding Seas, Estuaries and Coasts, 35(2), 369–382, doi:10.1007/s12237-011-9386-6, 2012.

722   Hugelius, G., Strauss, J., Zubrzycki, S., Harden, J. W., Schuur, E. A. G., Ping, C. L., Schirrmeister, L., Grosse, G.,
723   Michaelson, G. J., Koven, C. D., O'Donnell, J. A., Elberling, B., Mishra, U., Camill, P., Yu, Z., Palmtag, J. and
724   Kuhry, P.: Improved estimates show large circumpolar stocks of permafrost carbon while quantifying substantial
725   uncertainty ranges and identifying remaining data gaps, Biogeosciences Discussions, 11(3), 4771–4822,
726   doi:10.5194/bgd-11-4771-2014, 2014.

727   Ivanov, V. V. and Golovin, P. N.: Observations and modeling of dense water cascading from the northwestern
728   Laptev Sea shelf, Journal of Geophysical Research: Oceans, 112(9), 1–15, doi:10.1029/2006JC003882, 2007.

729   Jakobsson, M., Grantz, A., Kristoffersen, Y. and Macnab, R.: Physiography and Bathymetry of the Arctic Ocean,
730   in The Organic Carbon Cycle in the Arctic Ocean, edited by R. Stein and R. W. Macdonald, pp. 1–5., 2004.

731   Karlsson, E. S., Charkin, A., Dudarev, O., Semiletov, I., Vonk, J. E., Sánchez-García, L. and Andersson, A.:
732   Carbon isotopes and lipid biomarker investigation of sources, transport and degradation of terrestrial organic
733   matter in the Buor-Khaya Bay, SE Laptev Sea, Biogeosciences, 8(7), 1865–1879, doi:10.5194/bg-8-1865-2011,
734   2011.

735   Karlsson, E. S., Brüchert, V., Tesi, T., Charkin, a, Dudarev, O., Semiletov, I. and Gustafsson, Ö.: Contrasting
736   regimes for organic matter degradation in the East Siberian Sea and the Laptev Sea assessed through microbial
737   incubations and molecular markers, Marine Chemistry, 170, 11–22, doi:10.1016/j.marchem.2014.12.005, 2014.

738   Keil, R. G., Tsamakis, E., Fuh, C. B., Giddings, J. C. and Hedges, J. I.: Mineralogical and textural controls on the
739   organic composition of coastal marine sediments: Hydrodynamic separation using SPLITT-fractionation,
740   Geochimica et Cosmochimica Acta, 58(2), 879–893, doi:10.1016/0016-7037(94)90512-6, 1994.

741   Keil, R. G., Mayer, L. M., Quay, P. D., Richey, J. E. and Hedges, J. I.: Loss of organic matter from riverine
742   particles in deltas, Geochimica et Cosmochimica Acta, 61(7), 1507–1511, doi:10.1016/S0016-7037(97)00044-6,
743   1997a.

744   Keil, R. G., Tsamakis, E. and Wolf, N.: Relationships between organic carbon preservation and mineral surface
745   area in Amazon fan sediments (Holes 932A and 942A), Proceedings of the Ocean Drilling Program, 155, 531–
746   538 [online] Available from: http://cat.inist.fr/?aModele=afficheN&cpsidt=2169716, 1997b.

747   Keil, R. G., Dickens, A. F., Arnarson, T., Nunn, B. L. and Devol, A. H.: What is the oxygen exposure time of
748   laterally transported organic matter along the Washington margin?, Marine Chemistry, 92(1-4 SPEC. ISS.), 157–
749   165, doi:10.1016/j.marchem.2004.06.024, 2004.

750   Macdonald, R. W., Naidu, A. S., Yunker, M. B. and Gobeil, C.: The Beaufort Sea: distribution, sources, fluxes and
751   burial of organic carbon, in The Organic Carbon Cycle in the Arctic Ocean, edited by R. Stein and R. W.
752   Macdonald, pp. 177–192., 2004.

753   Magen, C., Chaillou, G., Crowe, S. a., Mucci, A., Sundby, B., Gao, A., Makabe, R. and Sasaki, H.: Origin and fate
754   of particulate organic matter in the southern Beaufort Sea - Amundsen Gulf region, Canadian Arctic, Estuarine,
755   Coastal and Shelf Science, 86(1), 31–41, doi:10.1016/j.ecss.2009.09.009, 2010.

756   Mammone, K. A.: Sediment provenance and transport on the Siberian Arctic shelf, Oregon State University.,
757   1998.

758   Mayer, L. M.: Surface area control of organic carbon accumulation in continental shelf sediments, Geochimica et
759   Cosmochimica Acta, 58(4), 1271–1284, doi:10.1016/0016-7037(94)90381-6, 1994.

760   McClelland, J. W., Holmes, R. M., Peterson, B. J., Amon, R., Brabets, T., Cooper, L., Gibson, J., Gordeev, V. V.,
761   Guay, C., Milburn, D., Staples, R., Raymond, P. A., Shiklomanov, I., Stiegl, R., Zhulidov, A., Gurtovaya, T. and
762   Zimov, S.: Development of a Pan-Arctic Database for River Chemistry From Corals to Canyons : The Great
763   Barrier Reef Margin, Program, 89(24), 217–218, doi:10.1029/2006JG000353., 2008.

Biogeosciences
Discussions

Open Access

EGU

764 Mercone, D., Thomson, J., Abu-Zied, R. H., Croudace, I. W. and Rohling, E. J.: High-resolution geochemical and
765 micropalaeontological profiling of the most recent eastern Mediterranean sapropel, Marine Geology, 177(1-2), 25–
766 44, doi:10.1016/S0025-3227(01)00122-0, 2001.

767 Meyers, P. A. and Ishiwatari, R.: Lacustrine organic geochemistry-an overview of indicators of organic matter
768 sources and diagenesis in lake sediments, Organic Geochemistry, 20(7), 867–900, doi:10.1016/0146-
769 6380(93)90100-P, 1993.

770 Naidu, A. S., Cooper, L. W., Finney, B. P., Macdonald, R. W., Alexander, C. and Semiletov, I. P.: Organic carbon
771 isotope ratio (d13C) of Arctic Amerasian Continental shelf sediments, International Journal of Earth Sciences,
772 89(3), 522–532, doi:10.1007/s005310000121, 2000.

773 Nieuwenhuize, J., Maas, Y. E. . and Middelburg, J. J.: Rapid analysis of organic carbon and nitrogen in particulate
774 materials, Marine Chemistry, 45(3), 217–224, doi:10.1016/0304-4203(94)90005-1, 1994.

775 Opsahl, S. and Benner, R.: Early diagenesis of vascular plant tissues : Lignin and cutin decomposition and
776 biogeochemical implications, Geochimica et Cosmochimica Acta, 59(23), 4889–4904, 1995.

777 Panova, E., Tesi, T., Pearce, C., Salvadó, J. A., Karlsson, E. S., Kruså, M., Semiletov, I. P. and Gustafsson, Ö.:
778 Geochemical compositional differences of the supramicron plankton-dominated fraction in two regimes of the
779 Marginal Ice Zone (MIZ) of the outer East Siberian Arctic Shelf, in AGU Fall Meeting, p. Conference Abstract
780 C43A–0797., 2015.

781 Pearson, A., Mcnichol, A. P., Schneider, R. J., von Reden, K. F. and Zheng, Y.: Microscale AMS 14C
782 measurement at NOSAMS, Radiocarbon, 40(1), 61–75, 1998.

783 Prahl, F. G., Ertel, J. R., Goni, M. A., Sparrow, M. A. and Eversmeyer, B.: Terrestrial organic carbon contributions
784 to sediments on the Washington margin, Geochimica et Cosmochimica Acta, 58(14), 3035–3048,
785 doi:10.1016/0016-7037(94)90177-5, 1994.

786 Rachold, V. and Hubberten, H. W.: Carbon isotope composition of particulate organic material in east Siberian
787 rivers, Land-Ocean Systems in the Siberian Arctic: Dynamics and History, 223–238, 1998.

788 Rachold, V., Grigoriev, M. N., Are, F. E., Solomon, S., Reimnitz, E., Kassens, H. and Antonow, M.: Coastal
789 erosion vs riverine sediment discharge in the Arctic Shelf seas, International Journal of Earth Sciences, 89(3),
790 450–459, doi:10.1007/s005310000113, 2000.

791 Rachold, V., Eicken, H., Gordeev, V. V, Grigoriev, M. N., Hubberten, H.-W., Lisitzin, A. P., Shevchenko, V. P. and
792 Schirrmeister, L.: Modern Terrigenous Organic Carbon Input to the \textsc{A}rctic \textsc{O}cean, The Organic
793 Carbon Cycle in the Arctic Ocean, 33–55, 2004.

794 Sakshaug, E.: Primary and secondary production in the Arctic Seas, in The Organic Carbon Cycle in the Arctic
795 Ocean, edited by R. Stein and R. W. Macdonald, pp. 57–81., 2004.

796 Salvadó, J. A., Tesi, T., Andersson, A., Ingri, J., Dudarev, O. V., Semiletov, I. P. and Gustafsson, Ö.: Organic
797 carbon remobilized from thawing permafrost is resequestered by reactive iron on the Eurasian Arctic Shelf,
798 Geophysical Research Letters, 42(19), 8122–8130, doi:10.1002/2015GL066058, 2015.

799 Sánchez-García, L., Alling, V., Pugach, S., Vonk, J., Van Dongen, B., Humborg, C., Dudarev, O., Semiletov, I.
800 and Gustafsson, Ö.: Inventories and behavior of particulate organic carbon in the Laptev and East Siberian seas,
801 Global Biogeochemical Cycles, 25(2), 1–13, doi:10.1029/2010GB003862, 2011.

802 Schubert, C. J. and Calvert, S. E.: Nitrogen and carbon isotopic composition of marine and terrestrial organic
803 matter in Arctic Ocean sediments:, Deep Sea Research Part I: Oceanographic Research Papers, 48(3), 789–810,
804 doi:10.1016/S0967-0637(00)00069-8, 2001.

805 Semiletov, I. and Gustafsson, Ö.: East Siberian Shelf Study Alleviates Scarcity of Observations, Eos,
806 Transactions American Geophysical Union, 90(17), 145, doi:10.1029/2009EO170001, 2009.

807 Semiletov, I., Dudarev, O., Luchin, V., Charkin, A., Shin, K. H. and Tanaka, N.: The East Siberian Sea as a
808 transition zone between Pacific-derived waters and Arctic shelf waters, Geophysical Research Letters, 32(10), 1–
809 5, doi:10.1029/2005GL022490, 2005.

810 Semiletov, I., Pipko, I., Gustafsson, Ö., Anderson, L. G., Sergienko, V., Pugach, S., Dudarev, O., Charkin, A.,
811 Gukov, A., Bröder, L., Andersson, A., Spivak, E. and Shakhova, N.: Acidification of East Siberian Arctic Shelf
812 waters through addition of freshwater and terrestrial carbon, Nature Geoscience, (April), doi:10.1038/NEGO2695,
813 2016.

814 Semiletov, I. P.: On aquatic sources and sinks of CO2 and CH4 in the Polar Regions, Journal of the Atmospheric
815 Sciences, 56(2), 286–306, 1999.

816 Semiletov, I. P., Pipko, I. I., Shakhova, N. E., Dudarev, O. V., Pugach, S. P., Charkin, A. N., Mcroy, C. P.,
817 Kosmach, D. and Gustafsson, Ö.: Carbon transport by the Lena River from its headwaters to the Arctic Ocean,
818 with emphasis on fluvial input of terrestrial particulate organic carbon vs. carbon transport by coastal erosion,
819 Biogeosciences, 8(9), 2407–2426, doi:10.5194/bg-8-2407-2011, 2011.

820 Semiletov, I. P., Shakhova, N. E., Sergienko, V. I., Pipko, I. I. and Dudarev, O. V: On carbon transport and fate in
821 the East Siberian Arctic land–shelf–atmosphere system, Environmental Research Letters, 7(1), 015201,
822 doi:10.1088/1748-9326/7/1/015201, 2012.

823 Shakhova, N., Semiletov, I., Sergienko, V., Lobkovsky, L., Yusupov, V., Salyuk, A., Salomatin, A., Chernykh, D.,
824 Kosmach, D., Panteleev, G., Nicolsky, D., Samarkin, V., Joye, S., Charkin, A., Dudarev, O., Meluzov, A. and
825 Gustafsson, O.: The East Siberian Arctic Shelf: towards further assessment of permafrost-related methane fluxes
826 and role of sea ice., Philosophical transactions. Series A, Mathematical, physical, and engineering sciences,
827 373(2052), 20140451–, doi:10.1098/rsta.2014.0451, 2015.

828 Stein, R. and Fahl, K.: Holocene accumulation of organic carbon at the Laptev Sea continental margin (Arctic
829 Ocean): sources, pathways, and sinks, Geo-Marine Letters, 20(1), 27–36, doi:10.1007/s003670000028, 2000.

830 Stein, R. and Fahl, K.: The Laptev Sea: Distribution, Sources, Variability and Burial of Organic Carbon, in The
831 Organic Carbon Cycle in the Arctic Ocean, edited by R. Stein and R. W. Macdonald, pp. 213–236., 2004.

832 Stein, R. and Macdonald, R. W., Eds.: The organic carbon cycle in the Arctic Ocean, Springer Verlag., 2004.

833 Stuvier, M. and Polach, H. A.: Reporting of 14C Data, Radiocarbon, 19(3), 355–363,
834 doi:10.1016/j.forsciint.2010.11.013, 1977.

835 Syvitski, J. P. M.: Sediment discharge variability in Arctic rivers: Implications for a warmer future, Polar Research,
836 21(2), 323–330, doi:10.1111/j.1751-8369.2002.tb00087.x, 2002.

837 Tarnocai, C., Canadell, J. G., Schuur, E. A. G., Kuhry, P., Mazhitova, G. and Zimov, S.: Soil organic carbon pools
838 in the northern circumpolar permafrost region, Global Biogeochemical Cycles, 23(2), 1–11,
839 doi:10.1029/2008GB003327, 2009.

840 Tesi, T., Semiletov, I., Hugelius, G., Dudarev, O., Kuhry, P. and Gustafsson, Ö.: Composition and fate of
841 terrigenous organic matter along the Arctic land-ocean continuum in East Siberia: Insights from biomarkers and
842 carbon isotopes, Geochimica et Cosmochimica Acta, 133, 235–256, doi:10.1016/j.gca.2014.02.045, 2014.

843 Tesi, T., Semiletov, I., Dudarev, O., Andersson, A. and Gustafsson, Ö.: Matrix association effects on
844 hydrodynamic sorting and degradation of terrestrial organic matter during cross-shelf transport in the Laptev and
845 East Siberian shelf seas, Journal of Geophysical Research: Biogeosciences, 121(3), 731–752,
846 doi:10.1002/2015JG003067, 2016.

847 van Dongen, B. E., Semiletov, I., Weijers, J. W. H. and Gustafsson, Ö.: Contrasting lipid biomarker composition of
848 terrestial organic matter exported from across the Eurasian Arctic by the five great Russian Arctic rivers, Global
849 Biogeochemical Cycles, 22(1), 1–14, doi:10.1029/2007GB002974, 2008a.

850 van Dongen, B. E., Zencak, Z. and Gustafsson, Ö.: Differential transport and degradation of bulk organic carbon
851 and specific terrestrial biomarkers in the surface waters of a sub-arctic brackish bay mixing zone, Marine
852 Chemistry, 112(3-4), 203–214, doi:10.1016/j.marchem.2008.08.002, 2008b.

853 Vonk, J. E. and Gustafsson, Ö.: Permafrost-carbon complexities, Nature Geoscience, 6(9), 675–676,
854 doi:10.1038/ngeo1937, 2013.

855 Vonk, J. E., Sánchez-García, L., Semiletov, I., Dudarev, O., Eglinton, T., Andersson, A. and Gustafsson, O.:
856 Molecular and radiocarbon constraints on sources and degradation of terrestrial organic carbon along the Kolyma
857 paleoriver transect, East Siberian Sea, Biogeosciences, 7(10), 3153–3166, doi:10.5194/bg-7-3153-2010, 2010.

858 Vonk, J. E., Sánchez-García, L., van Dongen, B. E., Alling, V., Kosmach, D., Charkin, A., Semiletov, I. P.,
859 Dudarev, O. V., Shakhova, N., Roos, P., Eglinton, T. I., Andersson, A. and Gustafsson, Ö.: Activation of old
860 carbon by erosion of coastal and subsea permafrost in Arctic Siberia, Nature, 489(7414), 137–140,
861 doi:10.1038/nature11392, 2012.

862 Vonk, J. E., Semiletov, I. P., Dudarev, O. V., Eglinton, T. I., Andersson, A., Shakhova, N., Charkin, A., Heim, B.
863 and Gustafsson, Ö.: Preferential burial of permafrost-derived organic carbon in Siberian-Arctic shelf waters,
864 Journal of Geophysical Research: Oceans, 119, 8410–8421, doi:10.1002/2014JC010261.Received, 2014.

Biogeosciences
Open Access
Discussions
EGU

865 Wegner, C., Hölemann, J. A., Dmitrenko, I., Kirillov, S. and Kassens, H.: Seasonal variations in Arctic sediment
866 dynamics - Evidence from 1-year records in the Laptev Sea (Siberian Arctic), Global and Planetary Change, 48(1-
867 3 SPEC. ISS.), 126–140, doi:10.1016/j.gloplacha.2004.12.009, 2005.

868 Wegner, C., Bauch, D., Hölemann, J. A., Janout, M. A., Heim, B., Novikhin, A., Kassens, H. and Timokhov, L.:
869 Interannual variability of surface and bottom sediment transport on the Laptev Sea shelf during summer,
870 Biogeosciences, 10(2), 1117–1129, doi:10.5194/bg-10-1117-2013, 2013.

871 Weingartner, T. J., Danielson, S., Sasaki, Y., Pavlov, V. and Kulakov, M.: The Siberian Coastal Current: A wind-
872 and buoyancy-forced Arctic coastal current, Journal of Geophysical Research, 104(C12), 29697,
873 doi:10.1029/1999JC900161, 1999.

874 Wiesenberg, G. L. B., Schwark, L. and Schmidt, M. W. I.: Improved automated extraction and separation
875 procedure for soil lipid analyses, European Journal of Soil Science, 55(2), 349–356, doi:10.1111/j.1351-
876 0754.2004.00601.x, 2004.

877 Winterfeld, M., Goñi, M. A., Just, J., Hefter, J. and Mollenhauer, G.: Characterization of particulate organic matter
878 in the Lena River Delta and adjacent nearshore zone, NE Siberia - Part 2: Lignin-derived phenol compositions,
879 Biogeosciences, 12, 2261–2283, doi:10.5194/bgd-11-14359-2014, 2015a.

880 Winterfeld, M., Laepple, T. and Mollenhauer, G.: Characterization of particulate organic matter in the Lena River
881 delta and adjacent nearshore zone, NE Siberia - Part I: Radiocarbon inventories, Biogeosciences, 12(12), 3769–
882 3788, doi:10.5194/bg-12-3769-2015, 2015b.

883 Yunker, M. B., Macdonald, R. W., Cretney, W. J., Fowler, B. R., Mclaughlin, F. A. and Bay, R. R. B.: Alkane,
884 terpene, and polycyclic aromatic hydrocarbon geochemistry of the Mackenzie River and Mackenzie shelf."
885 Riverine contributions to Beaufort Sea coastal sediment, , 57, 3041–3061, 1993.

886 Yunker, M. B., Macdonald, R. W., Veltkamp, D. J. and Cretney, W. J.: Terrestrial and marine biomarkers in a
887 seasonally ice-covered Arctic estuary — integration of multivariate and biomarker approaches, Marine Chemistry,
888 49(1), 1–50, doi:http://dx.doi.org/10.1016/0304-4203(94)00057-K, 1995.

889 Yunker, M. B., Belicka, L. L., Harvey, H. R. and Macdonald, R. W.: Tracing the inputs and fate of marine and
890 terrigenous organic matter in Arctic Ocean sediments: A multivariate analysis of lipid biomarkers, Deep-Sea
891 Research Part II: Topical Studies in Oceanography, 52(24-26), 3478–3508, doi:10.1016/j.dsr2.2005.09.008, 2005.
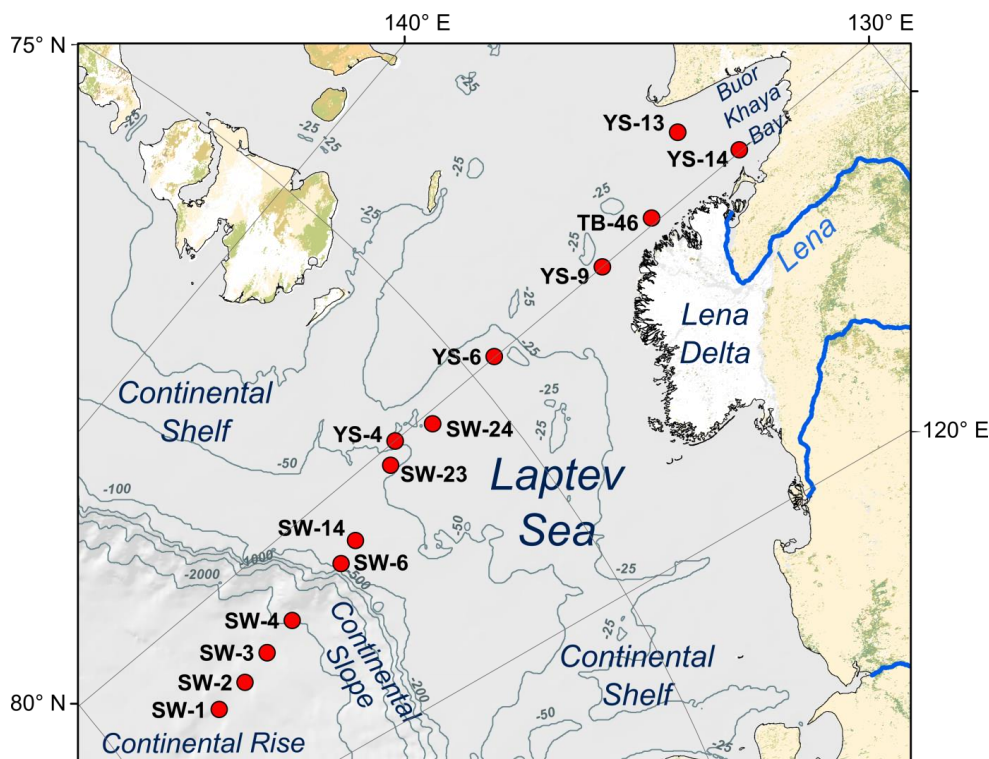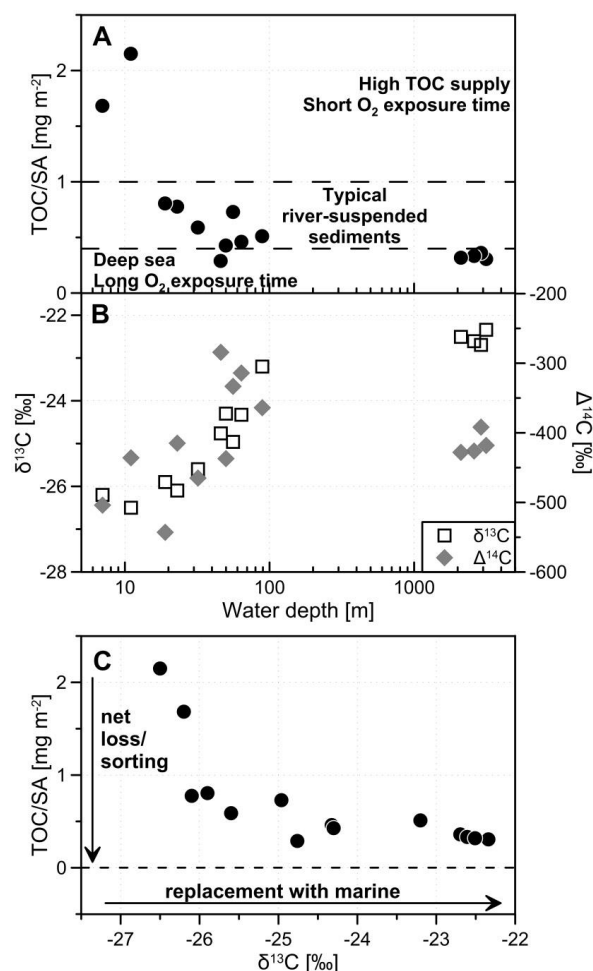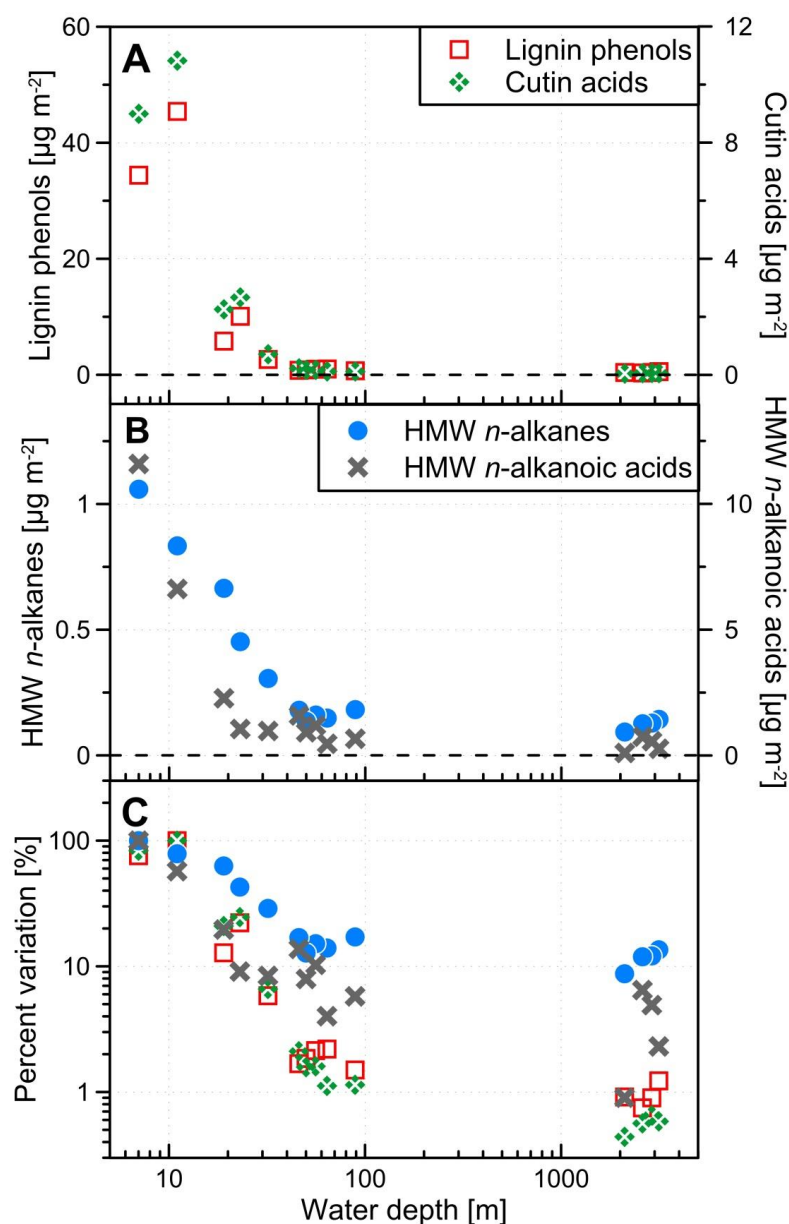
892

Figure 1: Map of the study area in the Laptev Sea. Red filled circles mark the sediment sampling sites. The transect reaches from the Lena River mouth and the Buor-Khaya Bay (water depths ~10 m) across the Laptev Sea Shelf (mean depth ~50 m) to the slope/shelf break and rise (water depths ~3000 m).
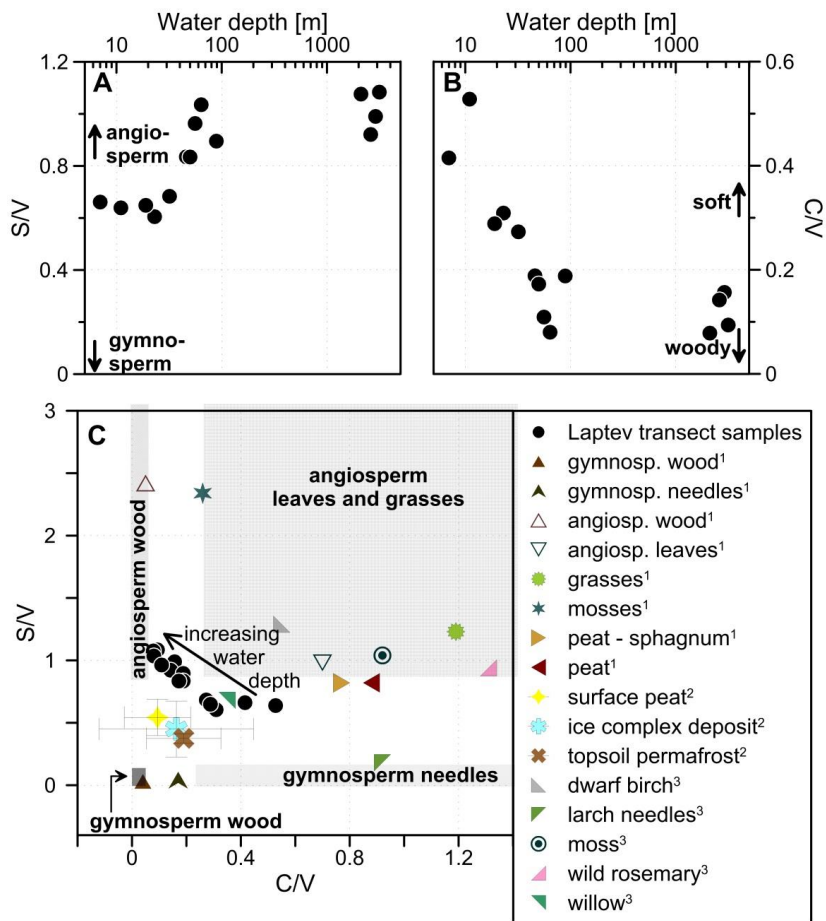
Biogeosciences
Discussions

EGU
Open Access

898

899 Figure 2: (A) The ratio of total organic carbon (TOC) to surface area (SA) decreases with

900 increasing water depth by a factor of 7 or 86%. (B) The stable carbon isotopic signal ($\delta^{13}C$)

901 increases with increasing water depth from -26 ‰ to -22 ‰, suggesting a change in source

902 material from terrigenous to marine dominated. The radiocarbon isotopic signal ($\Delta^{14}C$)

903 increases toward the outer shelf, supporting an increase in fresh marine organic carbon. The

904 slope sediments show an older (more depleted) $\Delta^{14}C$ signal, possibly due to ageing during

905 transport and in situ. (C) The relationship between TOC/SA and $\delta^{13}C$ can help to disentangle

906 two processes occurring simultaneously during cross-shelf transport: The net loss (i.e.

907 degradation) or sorting (i.e. hydraulically retaining) of TerrOC leads to a shift towards lower

908 TOC/SA ratios, whereas the replacement/dilution with marine OC shifts the isotopic signature

909 towards higher values.

Biogeosciences
Discussions

Open Access

EGU

910

Figure 3: Terrigenous biomarker loadings display a strong decrease with increasing water
depth: (A) for lignin phenols and cutin acids by a factor of 130 and 230 respectively, (B) for
HMW n-alkanes and HMW n-alkanoic acids by a factor of 12 and 44, respectively. (C)
Comparison between the different biomarkers along the transect: lignin phenols, cutin acids,
HMW n-alkanoic acids and n-alkanes where each is normalized to respective highest value
(corresponding to 100 %).

917

Figure 4: The lignin phenol composition carries source information: (A) an increasing ratio of
syringyl to vanillyl phenols (S/V) suggests relatively more angiosperm material on the outer
shelf/slope possibly due to selective degradation or sorting during transport. (B) The ratio of
cinnamyl to vanillyl phenols (C/V) decreases with increasing water depths, which implies an
increasing relative contribution of woody material compared to soft tissues. (C) Comparison
of S/V and C/V with the end-members for different Arctic plants as compiled from different
studies by Amon et al. (2012, and citations therein, here marked with [1]); ice-complex deposit
and topsoil permafrost as determined by Tesi et al. (2014, here marked with [2]) and more
plant species measured by Winterfeld et al. (2015a, here marked with [3]). The boxes indicate
typical ranges of S/V and C/V for different vascular plant tissues in different locations (e.g.
Goñi et al., 2000). The surface sediment lignin phenol compositions along the Laptev
transect appear to be a mix of angio- and gymnosperm soft tissues most similar to willow and
shift towards angiosperm wood with increasing water depth.

Figure 5: Degradation proxies for TerrOC, blue triangles point toward lower extent of degradation: (A) CuO-oxidation derived ratios Sd/Sl, Vd/Vl and 3,5-Bd/V all display a trend toward more degraded material with increasing distance from the shore with no difference between outer shelf and slope/rise sediments. (B) The carbon preference indices (CPI) of HMW n-alkanes and n-alkanoic acids show the same trend, yet not as pronounced for the n-alkanoic acids. The ratio of HMW n-alkanoic acids to HMW n-alkanes has a wider scatter, but also hints at more degraded material with increasing water depth.

940 **Table 1: List of surface sediment samples from the Laptev Sea transect.**

ID	Sample type	Lat	Long	Water depth	OC	SA	$\delta^{13}C$	$\Delta^{14}C$	SiO_2	Al_2O_3	CaO
		° N	° E	m	mg·g^{-1}	m^2·g^{-1}	‰	‰	wt %	wt %	wt %
SW-1	0-0.5cm	78.942	125.243	3146	10.4	34.0	-22.34	-418	60.3	16.5	2.4
SW-2	0-0.5cm	78.581	125.607	2900	13.8	38.3	-22.70	-392	57.8	17.2	2.1
SW-3	0-0.5cm	78.238	126.150	2601	10.6	31.8	-22.61	-426	62.1	16.0	1.6
SW-4	0-0.5cm	77.855	126.664	2106	13.2	41.5	-22.51	-428	56.6	17.5	1.3
SW-6	0-1cm	77.142	127.378	89	7.6	14.9	-23.20	-364	72.0	12.6	1.7
SW-14	0-1cm	76.894	127.798	64	8.9	19.4	-24.33	-314	71.3	12.5	1.5
SW-23	0-1cm	76.171	129.333	56	15.8	21.7	-24.96	-333	68.9	13.6	1.4
YS-4	0-1cm	75.987	129.984	50	13.4[a]	31.4	-24.76[a]	-284[a]	63.8	15.1	1.3
SW-24	0-1cm	75.599	129.558	46	10.7	37.0	-24.30	-437	62.5	15.4	1.2
YS-6	0-1cm	74.724	130.016	32	18.6[a]	31.6	-25.60[a]	-465[a]	62.1	16.1	1.3
YS-9	Grab	73.366	129.997	23	13.1[b]	16.9	-26.10[b]	-415[b]	70.8	14.0	1.3
YS-13	0-1cm	71.968	131.701	19	18.9[a]	23.5	-25.90[a]	-543[a]	61.6	17.4	0.8
YS-14	0-1cm	71.630	130.050	7	19.1[a]	11.4	-26.20[a]	-504[a]	69.6	15.0	1.6
TB-46	Grab	72.700	130.180	11	25.8[a]	12.0[c]	-26.50[a]	-436[a]	67.9	15.2	1.8

941

942   [a] Data from Vonk et al. (2012); [b] data from Tesi et al. (2016); [c] data from Karlsson et al.
943   (2014).

944   **Table 2: Biomarker results for surface sediment samples from the Laptev Sea**

945   **transect.**

ID	Lignin	Cutin	HMW* alkanes	HMW** acids	S/V	C/V	Sd/Sl	Vd/Vl	3,5Bd/V	CPI alk	CPI acids	acids/ alk
	µg m^{-2}	µg m^{-2}	µg m^{-2}	µg m^{-2}								
SW-1	0.56	0.063	0.14	0.27	1.1	0.09	1.3	0.98	0.43	2.5	4.1	1.9
SW-2	0.41	0.070	0.13	0.57	0.99	0.16	1.3	0.99	0.52	1.9	4.1	4.3
SW-3	0.34	0.061	0.13	0.75	0.92	0.14	1.3	0.95	0.61	1.7	4.1	6.0
SW-4	0.42	0.048	0.093	0.10	1.1	0.08	1.4	1.0	0.58	2.7	4.1	1.1
SW-6	0.68	0.12	0.18	0.67	0.90	0.19	1.2	1.0	0.46	2.9	4.4	3.7
SW-14	1.0	0.12	0.15	0.46	1.0	0.08	1.4	1.1	0.46	2.8	4.8	3.1
SW-23	0.97	0.17	0.16	1.2	0.96	0.11	1.3	1.1	0.48	3.2	4.4	7.4
YS-4	0.84	0.17	0.13	0.92	0.83	0.17	1.3	1.1	0.38	4.0	3.7	6.8
SW-24	0.76	0.23	0.18	1.6	0.84	0.19	1.2	1.1	0.43	4.0	3.9	8.9
YS-6	2.7	0.71	0.31	0.97	0.68	0.27	0.94	0.79	0.25	4.6	4.6	3.2
YS-9	10	2.7	0.45	1.1	0.60	0.31	0.65	0.60	0.16	4.7	4.1	2.3
YS-13	5.8	2.3	0.64	2.3	0.65	0.29	0.88	0.78	0.25	3.4	3.6	3.4
YS-14	34	9.0	1.1	12	0.66	0.42	0.57	0.50	0.11	6.0	5.9	11
TB-46	45	11	0.83[d]	6.6[d]	0.64	0.53	0.55	0.47	0.12	5.4[d]	5.0[d]	7.9[d]

946

947   * carbon chain-lengths 23-34; ** carbon chain-lengths 24-30.

948   [d] recalculated data from Karlsson et al. (2011).